

SCIENTIFIC REPORTS

OPEN

Comparison between *Listeria sensu stricto* and *Listeria sensu lato* strains identifies novel determinants involved in infection

Jakob Schardt¹, Grant Jones², Stefanie Müller-Herbst¹, Kristina Schauer³, Sarah E. F. D’Orazio² & Thilo M. Fuchs^{1,4}

The human pathogen *L. monocytogenes* and the animal pathogen *L. ivanovii*, together with four other species isolated from symptom-free animals, form the “*Listeria sensu stricto*” clade. The members of the second clade, “*Listeria sensu lato*”, are believed to be solely environmental bacteria without the ability to colonize mammalian hosts. To identify novel determinants that contribute to infection by *L. monocytogenes*, the causative agent of the foodborne disease listeriosis, we performed a genome comparison of the two clades and found 151 candidate genes that are conserved in the *Listeria sensu stricto* species. Two factors were investigated further *in vitro* and *in vivo*. A mutant lacking an ATP-binding cassette transporter exhibited defective adhesion and invasion of human Caco-2 cells. Using a mouse model of foodborne *L. monocytogenes* infection, a reduced number of the mutant strain compared to the parental strain was observed in the small intestine and the liver. Another mutant with a defective 1,2-propanediol degradation pathway showed reduced persistence in the stool of infected mice, suggesting a role of 1,2-propanediol as a carbon and energy source of listeriae during infection. These findings reveal the relevance of novel factors for the colonization process of *L. monocytogenes*.

Listeria monocytogenes is a Gram-positive, facultative anaerobic, non-sporulating, rod-shaped bacterium¹. The genus *Listeria* belongs to the phylum of Firmicutes, which is composed of Gram-positive bacteria with low GC-content (36–42%) and also includes the genera *Bacillus*, *Clostridium*, *Enterococcus*, *Streptococcus*, and *Staphylococcus*^{2,3}. *L. monocytogenes* is ubiquitous in nature and has been isolated from a variety of ecological niches, such as soil, vegetation, water, and feces⁴. It is a saprophyte that can live on decaying plant material. This prevalence in the environment is promoted by its ability to adapt to salt, acid, and temperature stresses. It can tolerate wide ranges of pH (pH 4.5–9.0) and temperature (0°C–45°C) and high concentrations of salt (up to 10% NaCl)⁵. In addition, it can form biofilms⁶. The persistence of certain *L. monocytogenes* strains in processing equipment poses a major challenge for the food industry⁷.

L. monocytogenes is the causative agent of the foodborne disease human listeriosis. Consumption of contaminated raw and industrially processed foods such as milk and other dairy products, meat products, vegetables, seafood, and ready-to-eat food is the main cause of infection¹. Clinical symptoms include gastroenteritis, meningitis, meningoencephalitis, septicemia and prenatal infection⁸. Listeriosis has a high mortality rate of up to 20–30% regardless of early antibiotic treatment, and infants, elderly and immunocompromised individuals are the main risk groups⁹. Upon ingestion, the pathogen encounters a variety of stressful conditions during the gastrointestinal passage, including acidic and osmotic stresses. It is believed that these physiological stresses serve as a signal for priming of the cell for invasion and an intracellular lifestyle^{10,11}. For example, acidic and osmotic stresses during passage through the stomach and small intestine trigger the expression of sigma factor B (σ^B), which induces

¹ZIEL-Institute for Food & Health, and Lehrstuhl für Mikrobielle Ökologie, Wissenschaftszentrum Weihenstephan, Technische Universität München, Weihenstephaner Berg 3, 85354, Freising, Germany. ²Department of Microbiology, Immunology, & Molecular Genetics, University of Kentucky, Lexington, Kentucky, USA. ³Lehrstuhl für Hygiene und Technologie der Milch, Tiermedizinische Fakultät, Ludwig-Maximilians-Universität München, Schönleutner Str. 8, 85764, Oberschleißheim, Germany. ⁴Friedrich-Loeffler-Institut, Institut für Molekulare Pathogenese, Naumburger Str. 96a, 07743, Jena, Germany. Correspondence and requests for materials should be addressed to T.M.F. (email: thilom.fuchs@fli.de)

several stress response- and virulence-associated genes^{12,13}. σ^B works synergistically with the positive regulatory factor A (PrfA), a thermo-regulated transcription factor active at 37 °C (the body temperature of the host) as well as at ambient temperatures upon induction by low pH¹⁴; this transcription factor controls expression of the main virulence genes¹⁵.

The genus *Listeria* currently consists of 17 species. The only other pathogenic member besides *L. monocytogenes* is *L. ivanovii*¹⁶, an organism that rarely infects humans^{17,18}, but frequently causes listeriosis in ruminants^{19,20}. Together with *L. marthii*²¹, *L. innocua*, *L. welshimeri*, and *L. seeligeri*, these two species form the “*Listeria sensu stricto*” group²², one of two distinct clades in the genus *Listeria*. All members of this clade (clade I) have been found in feces or the gastrointestinal tract of symptom-free animals, as well as in food of animal origin^{23–27}, suggesting a specific interaction of these species with mammalian hosts. Clade II, the “*Listeria sensu lato*” group, contains the species *L. fleischmanni*²⁸, *L. weihenstephanensis*²⁹, *L. rocourtia*³⁰, *L. aquatica*, *L. cornellensis*, *L. riparia*, *L. floridensis*, *L. grandensis*³¹, *L. grayi*, *L. newyorkensis*, and *L. booriae*³², which have been isolated from food-associated surfaces or the environment.

While the systemic phase of *L. monocytogenes* infection and the factors involved are well characterized, colonization of the gastrointestinal tract is still underinvestigated. Given that all *sensu stricto* strains have been found in the gut, but only two strains have been associated with human disease, we postulated that there may be bacterial genes encoded within clade I that promote growth or survival in the mammalian gastrointestinal tract. To identify novel listerial genes that could be involved in adhesion to the mucosal epithelium, metabolism, or chemotaxis and motility, we compared the genomes of the *Listeria sensu stricto*-group with the genomes of the environmental strains belonging to the *Listeria sensu lato* group. A total of 151 gene products were identified as being encoded by all *sensu stricto* strains, but absent from the strains of the *sensu lato* group. These factors that possibly contribute to the interaction of listeriae with mammals include the flagellum, the metabolic capabilities to utilize ethanolamine and 1,2-propanediol (1,2-PD), and a set of mainly functionally unknown proteins involved in regulation and transport processes. A putative transporter and the 1,2-PD degradation pathway were tested here for their function and their role during infection by *L. monocytogenes*.

Results

***Listeria* phylogenetic groups exhibit differences in colonization ability after oral infection in female BALB/c mice.** To analyze the proliferation of different species from the *Listeria sensu stricto* and *Listeria sensu lato* groups in the gastrointestinal tract and in other organs, female BALB/c mice were orally infected with $4\text{--}9 \times 10^8$ cell forming units (cfu) of the *Listeria sensu stricto* species *L. monocytogenes* and *L. welshimeri*, as well as the *Listeria sensu lato* species *L. aquatica* and *L. booriae*. The number of luminal *Listeria* in the ileum and colon was determined 2 days post infection (p.i.) (Fig. 1a and b). There were significantly lower cfu numbers of the three non-pathogenic species in both compartments in comparison with the cfu numbers of *L. monocytogenes* strain EGDe. The cfu values of *L. aquatica* and *L. welshimeri* were similar in the ileum. *L. booriae* was barely detectable in both compartments and showed significantly lower mean values in comparison to *L. welshimeri* in the colon, but not in the ileum.

The number of tissue-associated bacteria, that is, in the mucus, the epithelial layer, or the lamina propria (LP) of the gastrointestinal tract, was also analyzed (Fig. 1c and d). While *L. monocytogenes* was found in high numbers of $2.5\text{--}6.9 \times 10^3$ cfu, the three other species were not detectable in these tissues, confirming their non-pathogenic behavior as reported previously for *L. welshimeri* in mice after intravenous injection³³. As expected, *L. monocytogenes* could also reach the mesenteric lymph nodes and spread to the liver and spleen of infected mice (Supplementary Fig. 1).

The cfu/mg feces from stool samples taken 3 h p.i., 1 day p.i., and 2 days p.i. of the same mice were additionally analyzed. No significant difference in the cfu/mg feces was observed either immediately after infection or within 24 h of infection. In all cases, the number of cfu decreased 1000-fold, suggesting a species-independent initial clearance of listeriae shed in the feces. After an additional 24 h, *L. monocytogenes* persisted in stool pellets, but the number of cfu decreased significantly for the three non-pathogenic species (Fig. 1e). This effect was more pronounced in the *Listeria sensu lato* species. For example, for half of the mice fed *L. aquatica*, no cfu were detected, and only 1 of 6 mice fed *L. booriae* were still shedding *Listeria*.

Genome comparison between *Listeria sensu stricto* and *Listeria sensu lato* species reveals candidate genes for infection.

The findings described above prompted us to identify as yet unknown genes associated with gut colonization by a genome sequence comparison of 16 out of the 17 known *Listeria* species type strains (all except *L. grayi*). For this purpose, we calculated the percentage of predicted amino acid sequence identity for each *L. monocytogenes* protein against the proteins of the other 15 species within both clades. Gene products with at least 70% sequence homology amongst the *Listeria sensu stricto* species were chosen for further analysis, and filtered against gene products with less than 30% sequence homology amongst the *Listeria sensu lato* species. Although homology of >40% is suggestive of functional homologs³⁴, we chose the more stringent threshold to focus on the most robust candidate genes. The resulting Table 1 comprises 151 gene products that are present in all clade I species and absent (or significantly divergent) in clade II species. A majority of the gene products are involved in flagellar biosynthesis and the cobalamin (vitamin B₁₂)-dependent utilization of ethanolamine and 1,2-PD. The gain of these clusters has already been described as an evolutionary event that contributed to the taxonomic definition of clade I³⁵. Motility is well known to contribute to successful infection by *L. monocytogenes*^{36–40}. Many candidate genes are involved in cell wall and membrane biogenesis, transport processes, transcription, and signaling (Table 1). There is experimental evidence that many of the genes specific for listeriae of clade I contribute to virulence properties, thus validating our approach: Two of the factors involved in peptidoglycan biosynthesis, Lmo0703 and Lmo0717, have been demonstrated to be controlled by the listerial virulence regulators DegU⁴¹ and MogR³⁷. Among the transporters, we listed SvpA (Lmo2185) and

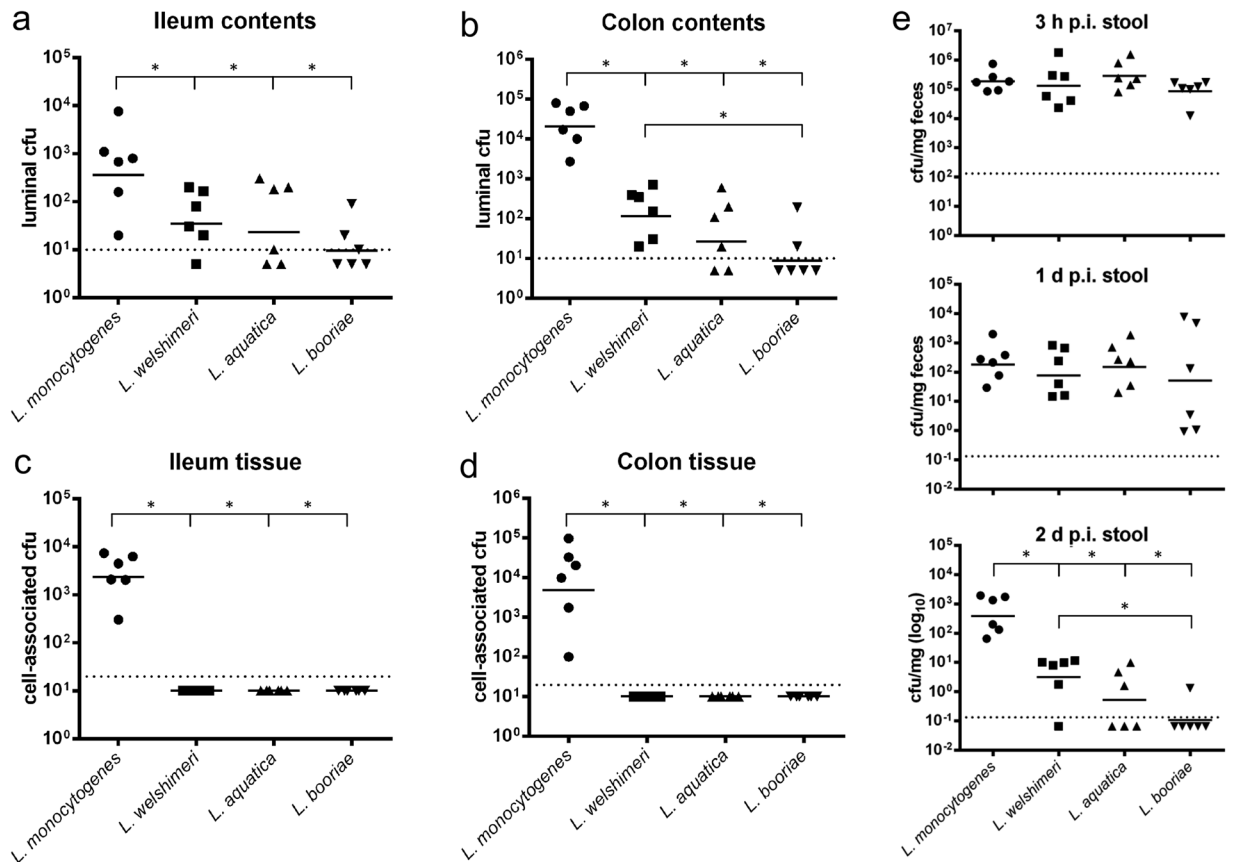


Figure 1. Members of the two listerial phylogenetic groups exhibit different cell numbers in the ileum and colon lumen. Female BALB/c mice were orally infected with $4\text{--}9 \times 10^8$ cfu of the *Listeria sensu stricto* species *L. monocytogenes* (●) and *L. welshimeri* (■), as well as of the *Listeria sensu lato* species *L. aquatica* (▲) and *L. booriae* (▼). After 2 days, cfu numbers for each species were determined in the ileum (a) and colon lumen (b), as well as in the ileum (c) and colon tissue (d). Stool samples (e) were collected at 3 h p.i., 1 day p.i. and 2 days p.i., and the number of cfu per mg feces was calculated. Symbols represent values for individual mice, while horizontal lines indicate the mean value that was pooled from two separate experiments ($n = 3$ mice per group). Dashed lines represent the detection limit for each sample. Statistical significance was assessed using two-tailed student's t-test with Welch's correction.

Lmo2186 with putative heme transport capacity. SpvA is a listerial virulence factor that promotes escape from phagosomes of macrophages⁴² and/or enables crossing of the digestive barrier⁴³. The ATPase synthase encoded by lmo0090-lmo0093 is known to play a role in intracellular survival⁴⁴, and deletion of the gene *pdeD* contributes to a decrease in listerial invasiveness in enterocytes⁴⁵. Because of their predicted, but not experimentally evaluated function *in vitro* or *in vivo*, we chose the putative ATP-binding cassette (ABC) transporter Lmo1131-1132 and the 1,2-PD utilization genes from Table 1 for further functional and infection experiments.

The operon lmo1131-1132 encoding a putative ABC transporter facilitates adhesion and invasion of *L. monocytogenes* in Caco-2 cells.

According to the Basic local alignment search tool on the NCBI homepage, the operon lmo1131-1132 encodes a putative ABC transporter. Both proteins Lmo1131 and Lmo1132 contain an ABC transporter-like transmembrane domain as well as a nucleotide binding domain. For further analysis of the functional role of the operon lmo1131-1132, we constructed the in-frame deletion mutant *L. monocytogenes* EGDe Δ lmo1131-1132 and tested adhesive and invasive capabilities in cell culture assays using Caco-2 (human colon carcinoma) cells and HEp-2 (human larynx squamous cell carcinoma) cells. Adhesion to Caco-2 cells was reduced in the deletion mutant compared with that of the parental strain EGDe by a factor of 2 (Fig. 2a). In contrast, cell culture assays with HEp-2 cells revealed no significant adhesion differences between EGDe and EGDe Δ lmo1131-1132 (Fig. 2b), suggesting a specific role of the ABC transporter in the interaction with Caco-2 cells. We also performed a gentamycin protection assay to test the invasion and the intracellular replication properties of the deletion mutant in Caco-2 and HEp-2 cells. Given that the number of intracellular cells detected 1 h after cell culture infection is a measure of the capacity of a strain to enter cells, we observed a more than 20-fold reduction of invasion of Caco-2 cells, but not of HEp-2 cells, by EGDe Δ lmo1131-1132 compared with that of the parental strain (Fig. 2c and d). The intracellular replication rates of EGDe [doubling time T_d (EGDe) = 83 min] and EGDe Δ lmo1131-1132 [T_d (EGDe Δ lmo1131-1132) = 83 min] however, were identical in the Caco-2 cells, indicating a specific role of the putative transporter in adhesion and/or invasion of this cell type.

gene name/lmo number	Function, protein name, or protein homology/similarity to	COG number	Gene name/lmo number	Function, protein name, or protein homology/similarity to	COG number
Metabolism			Miscellaneous		
lmo0661	Carboxymuconolactone decarboxylase family protein involved in protocatechuate catabolism	COG0599	lmo0090, 0091, 0093	ATP synthase α - γ -chain, ϵ -subunit; upregulated in Caco-2 cells and relevant for intracellular replication ^{44,62}	COG0056, 0224, 0355
<i>cobU-pduO</i> (lmo1141-1142, 1146-1148, 1169, 1190-1199, 1203-1209)	Cobalamin biosynthesis	COG2087	<i>pdeD</i> (lmo0111)	c-di-GMP-specific phosphodiesterase, EAL domain	COG2200
<i>pduS-pduQ</i> (lmo1143-1145, 1151-1171)	1,2-PD degradation pathway	COG4656	lmo0368	Putative Nudix hydrolase YfcD catalyzing the hydrolysis of nucleoside diphosphates	COG1443
<i>eutA-eutQ</i> (lmo1174-1187)	Ethanolamine utilization pathway	COG4819	lmo0481	Myosin-Cross-Reactive Antigen, oleate hydratase; upregulated <i>in vivo</i> ⁵⁷	COG4716
Cell motility and chemotaxis			lmo0511	Glutamine amidotransferase; DegU regulated	COG0518
<i>fliN-fliS</i> (lmo0675-lmo0718)	Flagellar biosynthesis	—	lmo0617	Putative lipoprotein with DUF4352 domain, immunoprotective extracellular protein ⁰²¹²	—
lmo0723, lmo1699	Methyl-accepting chemotaxis proteins	COG0840	lmo0625	Lipolytic protein GDSL family	COG2755
Cell wall/membrane/envelope biogenesis			lmo0635	2-Haloalkanoic acid dehalogenase with phosphatase activity	COG1011
lmo0703	UDP-N-acetylenolpyruvoylglucosamine reductase involved in peptidoglycan biosynthesis; regulated by DegU and MogR ^{88,89}	COG1728	lmo1415	Hydroxymethylglutaryl-CoA synthase involved in isopentenyl pyrophosphate synthesis via the mevalonate pathway; possibly influences V γ 9/V δ 2 T cells ⁹⁰	COG3425
lmo0717	Murein transglycosylase with N-acetyl-D-glucosamine binding site, SLT family; DegU and MogR regulated ^{88,89}	COG0741	lmo1638	Microcin C7 self-immunity protein MccF; its absence results in listerial accumulation in the liver ⁹¹	COG1619
lmo0724	Peptidase	COG4990	lmo2424	Thioredoxin	COG3118
Transporter			No orthologues		
lmo0269	Oligopeptide transport system permease protein	COG1173	lmo0615	Hypothetical protein	—
lmo0987	ABC transporter, permease protein, induced in CodY mutant ⁹² ; related to CylB of <i>Streptococcus agalactiae</i> involved in hemolysin production	COG1511	lmo0622	Hypothetical protein	—
lmo1131, 1132	ABC transporter, ATP-binding/permease protein	COG4988	lmo0657	Hypothetical protein	—
lmo2181	NPQTN specific sortase B; surface protein transpeptidase involved in anchoring of SvpA and Hbp1	COG4509	lmo0793	Putative transport protein	COG1811
<i>svpA/hbp2</i> (lmo2185), <i>hbp1</i> (lmo2186)	NPQTN cell wall anchored proteins with similarity to IsdA, IsdC of <i>Staphylococcus aureus</i> ⁹³ ; heme-binding NEAT domain associated with iron/heme transport ⁹⁴ ; Fur and MecA regulated virulence factor ^{32,43}	COG5386	lmo0819	Hypothetical protein	—
lmo2669	Type IV ABC-transporter, upregulated under anaerobic conditions ⁸⁰	COG4905	lmo1626	Hypothetical protein	—
Transcription			lmo1779	Hypothetical protein	—
lmo0212	Acetyltransferase, GNAT family	COG0456	lmo2063	Hypothetical protein	—
lmo1309, 1310	Co-activators of prophage gene expression IbrB, IbrA	COG1475, COG3969	lmo2065	Hypothetical protein	—
lmo1311	SNF2 family domain protein	COG0553	lmo2066	Hypothetical protein	—
lmo2234	Sugar phosphate isomerase	COG1082	lmo2169	Hypothetical protein	—
			lmo2432	Hypothetical protein; Fur-box ⁴³	—
			lmo2803	Hypothetical protein	—
			lmo2843	Hypothetical protein	COG5279

Table 1. Genes unique to *Listeria sensu stricto* strains and absent in *Listeria sensu lato* strains.

Transcription of lmo1131-1132 shows oxygen- and temperature-dependent regulation. We then examined the transcription of lmo1131 and lmo1132 in *L. monocytogenes* EGDe at 24 °C and 37 °C under both aerobic and anaerobic growth conditions via quantitative real time (qRT)-polymerase chain reaction (PCR) (Fig. 3). The two transporter genes exhibited similar transcription levels under all four conditions, suggesting transcription of the operon from a common promoter located upstream of lmo1131. Setting the transcriptional level of both genes at 37 °C with oxygen as 100%, we observed a decrease of the lmo1131 and lmo1132 mRNA

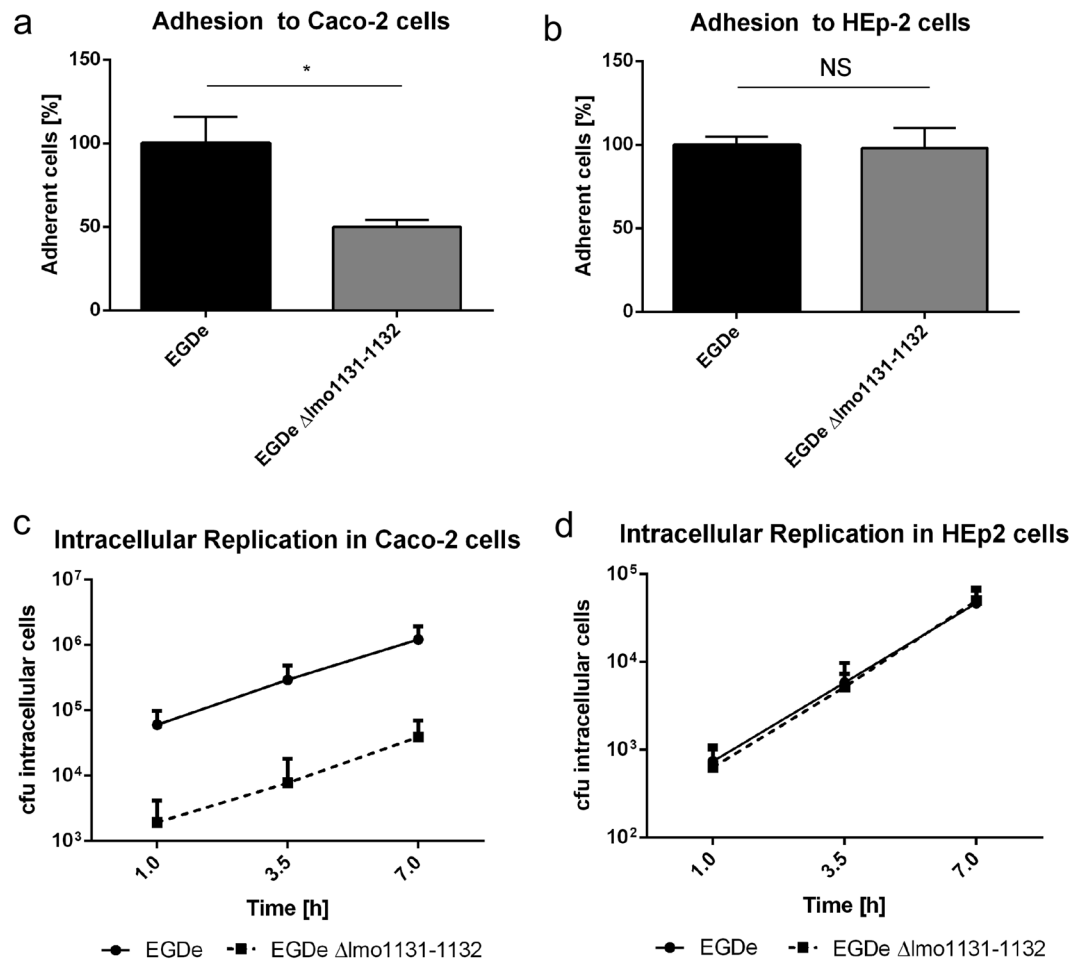


Figure 2. Adhesion to and invasion of Caco-2 and HEp-2 cells by a transporter mutant. The percentage of adherent cells of *L. monocytogenes* EGDe and EGDe Δ lmo1131-1132 to approximately 2.5×10^5 eukaryotic Caco-2 cells (a) or HEp-2 cells (b) was analyzed for a MOI of 10. The number of adherent EGDe cells was set to 100%. (c,d) The percentage of invasive and replicating cells of *L. monocytogenes* EGDe and EGDe Δ lmo1131-1132 was determined. Approximately 2.5×10^5 eukaryotic Caco-2 or HEp-2 cells were infected with a MOI of 10, and the numbers of intracellular bacterial cells were determined 1, 3.5 and 7 h p.i. Error bars indicate the standard deviation of three biologically independent experiments including technical replicates. Statistical significance was assessed using two-tailed student's t-test with Welch's correction; NS, not significant.

levels at 37°C to 4.77% and 6.15%, respectively, upon oxygen depletion. At 24°C, the transcription of the transporter genes was reduced to 55.80% and 64.02%, respectively, under aerobic conditions and to 3.18% and 4.53% in the absence of oxygen.

Lack of lmo1131-1132 leads to attenuated colonization of BALB/c mice. To verify the relevance of the candidate genes for the *in vivo* infection process, a food-borne transmission model in mice was used to enable study of the gastrointestinal phase of listeriosis⁴⁶. We conducted co-infection experiments with female BALB/c mice aged 6–8 weeks using a 1:1 ratio of EGDe and its mutant EGDe Δ lmo1131-1132 lacking the putative transporter genes. The strains were chromosomally tagged with pIMC3kan (EGDe) and pIMC3ery (mutant). Mice were fed a total of 1×10^9 cfu/mouse and the number of *Listeria* in the lumen of either the ileum or the colon was analyzed 2 days p.i. (Fig. 4a and b). The colon contained 25-fold more *L. monocytogenes* than the ileum, as was previously reported by others^{46,47}. However, there was no significant difference in the ratio of the two strains recovered from the intestinal contents of either tissue.

We then assessed the numbers of cfu associated with the flushed tissue, which includes *L. monocytogenes* trapped in the mucus layer, bacteria adhered to or inside intestinal epithelial cells (ECs) and bacteria that have reached the underlying LP. In both the ileum and the colon, a bimodal distribution was observed, with little or no *L. monocytogenes* recovered in approximately half of the mice, and up to 10^4 cfu in the other half (Fig. 4c). In the ileum, the average number of cfu for the latter group was six-fold higher for wildtype EGDe compared with the mutant. Overall, the competitive index (CI) revealed that the wild type strain outcompeted the mutant strain six-fold in the ileum (Fig. 4d). Interestingly, there was no significant difference between EGDe and EGDe Δ lmo1131-1132 in the colon.

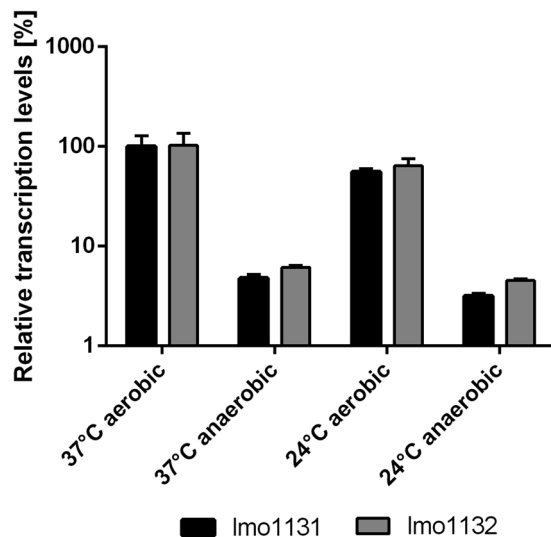


Figure 3. Temperature- and oxygen-dependent transcription of lmo1131 and lmo1132. Relative transcription of genes lmo1131 (black bars) and lmo1132 (gray bars) for the conditions 37 °C anaerobic, 24 °C aerobic, and 24 °C anaerobic was compared to that at 37 °C aerobic (preassigned as 100% gene expression for lmo1131). The results were calculated using the $2^{-\Delta\Delta CT}$ method⁹⁵ and lmo1759 (*pcrA*) was used as a reference gene for normalization. Error bars indicate the standard error of three biologically independent experiments including technical duplicates for each condition.

To further investigate this difference in intestinal colonization, the gut tissues of infected mice were fractionated, and the number of cfu in either the mucus layer, ECs or the LP were determined (Supplementary Fig. 2a). The number of wild type and EGDe Δ lmo1131-1132 in the mucus and the epithelial layer of the ileum did not differ significantly. However, wild type *L. monocytogenes* outnumbered the deletion mutant by five-fold in underlying LP of the ileum, similar to what was observed for whole tissue. As expected, there were no differences in the competitive indexes for any of the colon fractions. To assess the systemic spread of both strains, we also determined the bacterial load in the mesenteric lymph nodes (MLN), spleen and liver 2 days p.i. As shown in Fig. 4e and f, five-fold fewer EGDe Δ lmo1131-1132 were recovered from the liver compared to the wild type strain. There was no significant difference between the two strains in the MLN or the spleen. To test whether dissemination of the transporter mutant to peripheral organs was impaired or if the mutant strain had a specific growth defect in the liver, mice were intravenously injected with a 1:1 mixture of EGDe and EGDe Δ lmo1131-1132, and the total cfu in liver and spleen were determined 2 days p.i. Approximately equal numbers of both strains were recovered from the liver when the transmission route bypassed the gut (Supplementary Fig. 2b). Together, these data suggest that the transporter Lmo1131-1132 is involved in efficient translocation across the intestinal mucosa in the small intestine, but not the large intestine.

The *pduD* gene of *L. monocytogenes* is required for growth with 1,2-PD. Three large gene clusters responsible for the cobalamin-dependent utilization of ethanolamine and 1,2-PD were identified to be specific to the clade *sensu stricto* species of the genus *Listeria*²² (Table 1). These pathways have been demonstrated to play a role in the proliferation of *S. Typhimurium* *in vitro* and *in vivo*⁴⁸⁻⁵⁰, whereas no such experimental data have been available for *L. monocytogenes*. To investigate the role of 1,2-PD as a potential carbon and energy source for *L. monocytogenes*, strain EGDe and its mutant EGDe Δ *pduD*, which lacks a gene essential for 1,2-PD utilization, were grown in minimal medium⁵¹ (MM) without glucose, but with 0.5% (w/v) yeast extract under anaerobic conditions at 37 °C. No significant differences in the growth behavior of the two strains were observed. However, when we added 1,2-PD and cobalamin, which is an essential cofactor of PduCDE and whose biosynthesis is encoded by the *cob/cbi* gene cluster, EGDe grew to an optical density (OD)₆₀₀^{max} = 0.35, whereas the cell density of EGDe Δ *pduD* did not exceed that in the medium without 1,2-PD (Fig. 5a). Therefore, it might be speculated that all nutrients preferred over 1,2-PD are used up during the first 4 h, and that *L. monocytogenes* only then degrades 1,2-PD to reach a higher cell density.

As a control, we compared the growth of both strains in MM containing 50 mM glucose in the absence and presence of 1,2-PD and cobalamin. Under these growth conditions with glucose as an energy source, the addition of 1,2-PD had no significant effect on the cell density of either EGDe or EGDe Δ *pduD* (Fig. 5b), suggesting that 1,2-PD is utilized by *L. monocytogenes* only in the absence of glucose.

Supplementation with 1,2-PD and/or cobalamin leads to induction of *pdu* and *cob/cbi* genes during the stationary phase. To investigate the transcriptional response of the *pdu* and the *cob/cbi* gene clusters to the presence of 1,2-PD and/or cobalamin, a global transcriptome analysis of *L. monocytogenes* EGDe was conducted via next-generation sequencing (NGS). During growth in brain heart infusion (BHI) medium, in BHI medium with 10 mM 1,2-PD, or in BHI medium with 10 mM 1,2-PD and 25 nM cobalamin, cells were harvested in the mid-logarithmic (exponential) and stationary phases. During the exponential phase, the *pdu*

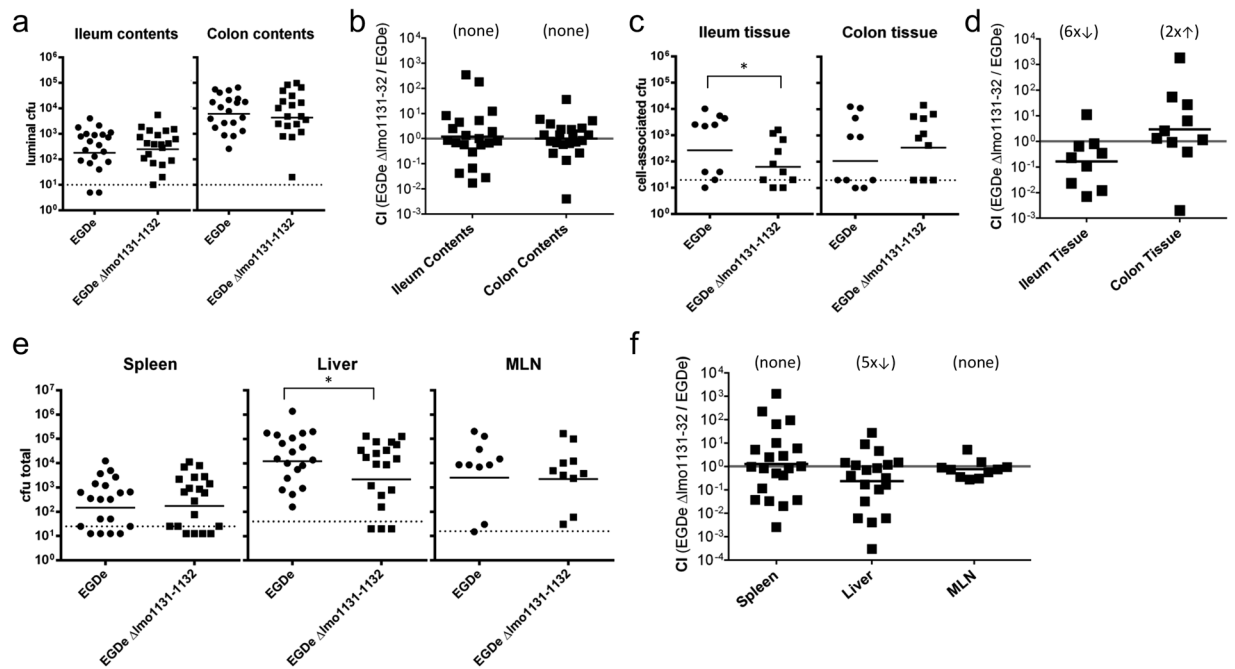


Figure 4. Deletion of *lmo1131-1132* leads to attenuated colonization of BALB/c mice. Female BALB/c mice were orally infected with a 1:1 ratio of *L. monocytogenes* EGDe and EGDe Δ lmo1131-1132 for a total inoculum of 1×10^9 cfu. After 2 days, the cfu of luminal (a) or cell-associated (c) strains in the ileum and colon were determined using kanamycin- (EGDe) or erythromycin (mutant)-containing plates, and the CI was calculated (b,d). (e) The cfu numbers of both strains in the spleen, liver and MLNs are shown. The numbers of EGDe (circles) or EGDe Δ lmo1131-1132 (squares) recovered in each mouse after co-infection are depicted. Solid horizontal lines indicate mean values, which were pooled from at least two separate experiments, while dashed lines represent the detection limit for each sample. (f) The CIs of the strains recovered from the organs are depicted. The geometric mean for each group was compared to the theoretical value of 1.0, and the fold change difference is indicated in parentheses. Statistical significance was assessed using two-tailed student's t-test with Welch's correction.

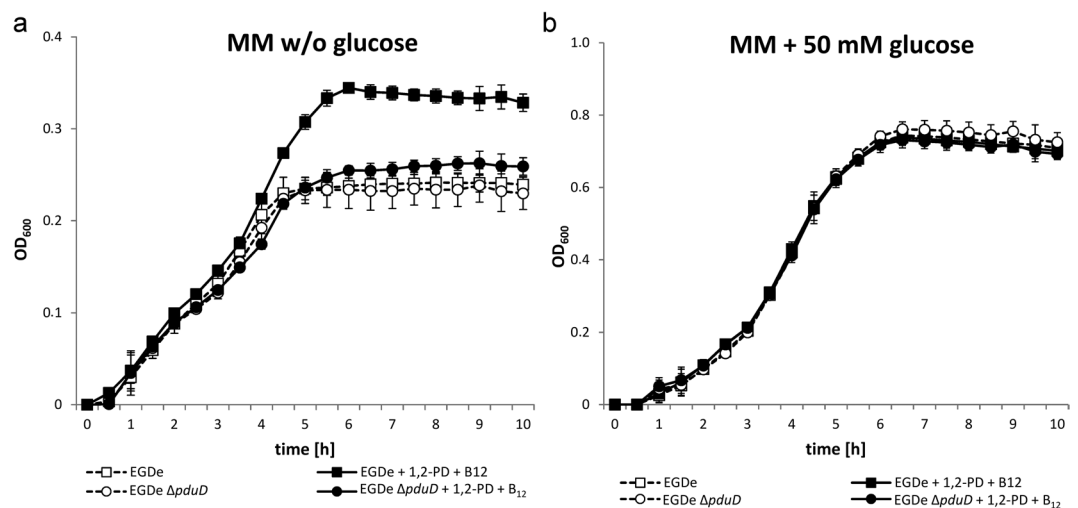


Figure 5. Improved growth of *L. monocytogenes* by addition of 1,2-PD. Growth curves of *L. monocytogenes* EGDe (□) and *L. monocytogenes* EGDe Δ pduD (○) in MM and 0.5% (w/v) yeast extract without glucose (a) or with 50 mM glucose (b) cultivated at 37°C under anaerobic conditions. MM was supplemented with 10 mM 1,2-PD and 25 nM cobalamin (filled symbols) or not supplemented (open symbols). OD₆₀₀ was measured at the indicated intervals using Bioscreen C. Growth curves depict the calculated mean value of three independent biological experiments with technical duplicates, while error bars indicate the standard deviation.

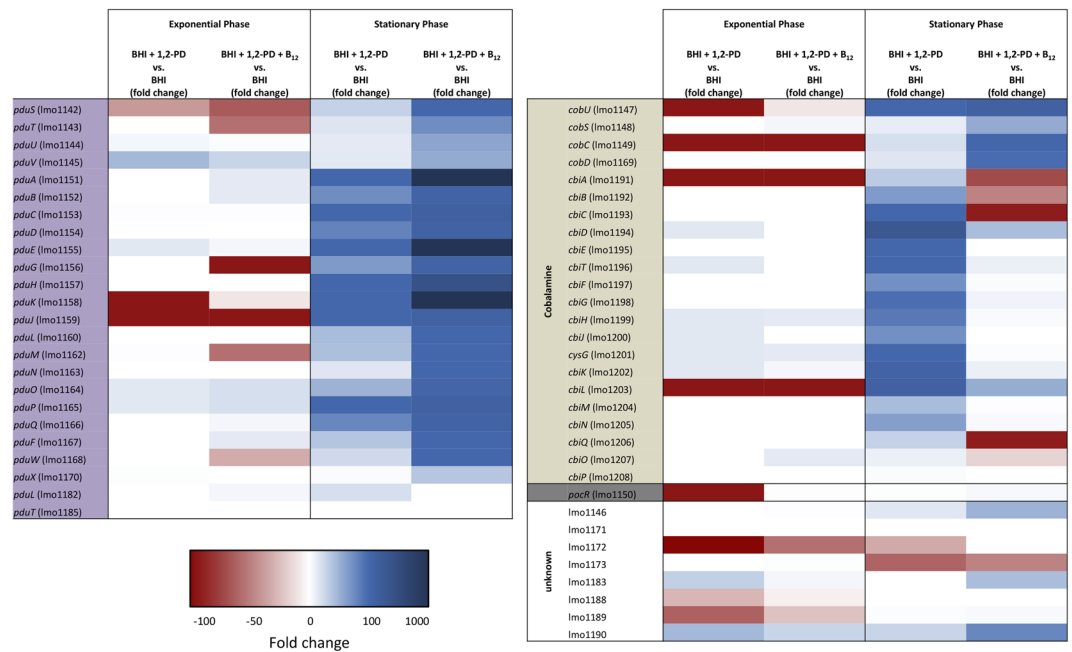


Figure 6. Transcriptome in response to growth with 1,2-PD. *L. monocytogenes* EGDe grown under different conditions was harvested during the exponential and stationary phases and the mRNA expression profile was analyzed via NGS using the Illumina MiSeq sequencing platform. Fold changes of normalized RPKM (reads per kilobase per million mapped reads) values under the conditions BHI with 10 mM 1,2-PD (BHI + 1,2-PD) and BHI with 10 mM 1,2-PD and 25 nM cobalamin (BHI + 1,2-PD + B₁₂) in comparison to BHI were calculated for both growth phases. The results were visualized using a three-color scheme with red colors indicating negative and blue colors indicating positive fold changes; white means no change. The color intensity corresponds to the magnitude of fold change. Unknown genes refer to genes located in the region of propanediol, ethanolamine, and cobalamin clusters without any known function.

and the *cob/cbi* gene clusters showed only weak or no transcription under all three growth conditions. During the stationary phase, transcription of these genes only slightly increased in BHI medium, although levels were still very low (Supplementary Table S1). However, when 1,2-PD was added to the cultures, a strong increase of expression of most *pdu* and *cob/cbi* genes in the range from two-fold to 1,605-fold induction was observed (Fig. 6). The transcription of *pdu* genes was even more elevated (up to more than 10,942-fold) when cobalamin was added, and the presence of this cofactor in the medium resulted in repression of the genes responsible for its biosynthesis (Supplementary Table S1), a finding that confirms a regulatory model in which the presence of cobalamin represses its own synthesis post-transcriptionally via stabilization of an mRNA hairpin⁵². The transcription levels of *pocR*, the regulator of both clusters, were only slightly elevated under medium supplemented with 1,2-PD and/or cobalamin. The *eut* genes of the ethanolamine degradation cluster, which are positioned between the *pdu* and *cbi/cob* clusters, were not significantly induced under the growth conditions applied (Supplementary Table S1).

The transcriptome data were successfully validated via qRT-PCR for the selected genes lmo1146, *pocR* (lmo1150), *pduC* (lmo1153), lmo1190 and *cbiA* (lmo1199) in stationary phase (Table 2). In exponential phase, there is a discrepancy between qRT-PCR and NGS results due to the higher sensitivity of qRT-PCR and the overall low number of RPKM values from the NGS (Suppl. Table S1). The results of both the transcriptome analysis and the qRT-PCR are compatible with the observation that the addition of 1,2-PD and cobalamin to *L. monocytogenes* EGDe in MM led to a growth advantage after exponential phase when other nutrients had been used up (Fig. 5a).

Deletion of *pduD* leads to faster clearance in BALB/c mice. We hypothesized that the ability to metabolize 1,2-PD would enhance the ability of *L. monocytogenes* to compete with gut microbiota and to persist in the intestinal lumen following oral transmission. To test this, female BALB/c mice were co-infected with a 1:1 ratio of wild type EGDe and an isogenic $\Delta pduD$ mutant (total of 1×10^9 cfu/mouse) that were differentially tagged with antibiotic resistances. Stools were collected daily for up to 14 days p.i., and the total number of strain per mg of feces was determined. As expected, a significant portion of the inoculum was shed in feces within 3 hours after feeding the mice, and the number of cfu detected 21 hours later had decreased considerably (Fig. 7a). At each time point after that, the average number of $\Delta pduD$ mutant bacteria recovered was less than the wildtype strain. By 10 days post-infection, the $\Delta pduD$ mutant had been cleared, but wildtype bacteria continued to be shed in the feces in at least some of the mice for up to 4 more days. Accordingly, the competitive index decreased steadily over the course of the experiment with a maximum difference on day 8 when the wild type bacteria out-competed the mutant bacteria by nearly 40-fold (Fig. 7b). Thus, the presence of the genes encoding the 1,2-PD utilization pathway prolonged the survival of *L. monocytogenes* EGDe in the mouse gastrointestinal tract.

Gene		Stationary Phase			Exponential Phase		
		BHI*	BHI + 1,2-PD	BHI + 1,2-PD + B ₁₂	BHI	BHI + 1,2-PD	BHI + 1,2-PD + B ₁₂
lmo1146	qRT-PCR	100	1,845	6,664	250	454	578
	NGS	100	1,623	5,038	49	50	90
lmo1150	qRT-PCR	100	421	1,137	84	111	108
	NGS	100	261	566	21	1	48
lmo1153	qRT-PCR	100	9,078	148,856	51	101	205
	NGS	100	12,377	77,536	25	50	45
lmo1190	qRT-PCR	100	20,583	52,177	70	216	288
	NGS	100	2,874	7,905	2	75	45
lmo1199	qRT-PCR	100	7,291	697	536	915	184
	NGS	100	8,724	486	3	50	45

Table 2. Relative transcription in percent of the genes *lmo1146*, *pocR* (*lmo1150*), *pduC* (*lmo1153*), *lmo1190* and *cbiH* (*lmo1199*) during growth in BHI with 10 mM 1,2-PD (BHI + 1,2-PD), in BHI with 10 mM 1,2-PD and 25 nM cobalamin (BHI + 1,2-PD + B₁₂), or in BHI. *The transcriptional activity obtained in the stationary phase of growth with BHI was set as 100% for each gene.

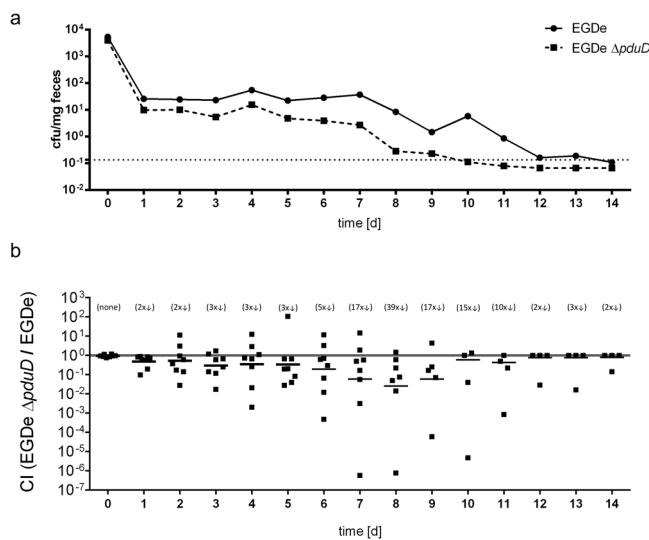


Figure 7. Deletion of *pduD* leads to faster clearance in BALB/c mice. Female BALB/c mice were orally infected with a 1:1 ratio of *L. monocytogenes* EGDe and EGDe $\Delta pduD$ for a total inoculum of 1×10^9 cfu. Stool samples were collected 3 h p.i. as well as every 24 h up to 16 days and the mean value of cfu per mg feces was calculated (a). Symbols represent mean values from two separate experiments ($n = 4$ mice per group) for *L. monocytogenes* EGDe (circles) and EGDe $\Delta pduD$ (squares) and dashed line represents the limit of detection. (b) CIs depict the ratio of EGDe $\Delta pduD$ /EGDe. The geometric mean for each group was compared to the theoretical value of 1.0 and the fold change difference is indicated in parentheses.

Discussion

It is believed that a common ancestor of the *Listeria sensu stricto* group took up a set of virulence genes through horizontal gene transfer, and that these determinants were subsequently lost in the non-pathogenic species of this listerial clade I^{53,54}. Other putative evolutionary processes differentiating *Listeria sensu stricto* from *Listeria sensu lato* are the expansion of internalin genes and the acquisition of the metabolically relevant *eut/pdu/cbi/cob* gene cluster as well as of flagellar genes, which were probably taken up via horizontal gene transfer from an ancestor of the *Bacillus cereus* complex²². The association of *Listeria sensu stricto* with fecal samples or the gastrointestinal tract of mostly symptom-free animals or food from animal origins^{23–27}, a reduced colonization rate of the environmental species *L. fleischmannii* and *L. floridensis* compared to *Listeria sensu stricto* species in fecal samples from wild rodents⁵⁵, as well as the alleviated colonization abilities of the *Listeria sensu lato* species in our BALB/c infection experiments, prompted us to speculate that a genome comparison of clade I versus clade II strains might identify as yet unknown listerial factors that play a role particularly during the gastrointestinal phase of infection.

Mice and other animal model organisms are considerably more resistant to oral infections than humans, and larger inocula need to be administered (10^9 – 10^{11} cfu/animal) to cause an intestinal infection⁵⁶. A high species specificity of the surface proteins InlA, which interacts well with ECs of humans or guinea pigs, but not with ECs of mice^{57,58}, contributes to inefficient oral transmission. Recent studies also show that competition with gut microbiota may limit opportunities for *L. monocytogenes* to invade the gut mucosa^{47,59}. To investigate the

relevance of as yet unknown listerial determinants for the gastrointestinal phase of listeriosis in more detail, we used a recently established and highly reproducible feeding model to mimic the natural course of infection⁴⁶ that overcomes the lack of reproducibility encountered by the conventional administration of listeriae by oral gavage.

Gastrointestinal infection is a multifactorial process and, besides the already mentioned stress conditions, metabolism is one of the key factors of pathogenic bacteria that can only survive in the intestine by searching for a specific niche providing sufficient amounts of nutrients⁶⁰. A hallmark of pathogens is therefore their metabolic flexibility during infection. Examples of this for *L. monocytogenes* include the utilization of sugar phosphates and glycerol as alternative carbon sources during intracellular replication^{61–63}, the requirement of both thiamine uptake and biosynthesis of thiamine precursors⁶⁴, or the possible exploitation of uncommon nitrogen sources such as ethanolamine or glucosamine⁶⁵. *L. monocytogenes* possesses a 53-kb island harboring genes for the metabolism of 1,2-PD, ethanolamine, and cobalamin, which can be found in all *Listeria sensu stricto* species²². These compounds can be found in the gastrointestinal tracts of animals and have been shown to play an important role in *Salmonella* pathogenesis^{49,66,67}. It has been discussed whether these gene clusters are also relevant for the virulence of listeriae, particularly for colonization⁵⁴. So far, it has been shown that ethanolamine utilization contributes to intracellular replication in ECs⁶², and that 1,2-PD is metabolized by *L. innocua*⁶⁸. Transcriptional studies in gnotobiotic mice infected with *L. monocytogenes* showed upregulation of most *pdu* genes during infection compared to growth in BHI⁶⁹. Our study not only demonstrates that *L. monocytogenes* can use 1,2-PD as a nutrient but also provides strong experimental evidence that the ability of *L. monocytogenes* to catabolize 1,2-PD contributes to its persistence and proliferation during gastrointestinal infection. This is in line with the finding that *S. Typhimurium* expansion is driven by 1,2-PD and that its utilization requires not only intestinal inflammation, but also the presence of commensal bacteria⁵⁰. These are assumed to provide 1,2-PD, for example, by the fermentation of fucose that has been cleaved from the mucosal glycans by commensal bacteria^{70,71}.

Toledo-Arana and colleagues showed that *lmo1131* but not *lmo1132* expression is decreased in intestinal *L. monocytogenes* of gnotobiotic mice compared with that under BHI growth conditions⁶⁹. Their reduced transcription at 24 °C and under anaerobic conditions suggests a role in an early stage of infection. A typical prokaryotic ABC transporter is composed of two hydrophobic transmembrane domains (TMDs) and two water soluble nucleotide binding domains (NBDs) at the cytosolic side of the cell membrane. An ABC transporter can be composed of four separate polypeptides, or two identical NBDs and/or TMDs can be present. NBDs and TMDs can also be fused together thus making up either the complete transporter from a single polypeptide or from two homo- or heterodimeric polypeptides⁷². *lmo1131* and *lmo1132* seem to belong to the group of “half transporters”, with two heterodimeric halves, each containing one NBD and one TMD. In addition to import functions, ABC transporters are involved in sorting molecules to the outer membrane. These molecules include lipoproteins, polysaccharides or fimbriae that might contribute to the interaction with mammalian cells^{73,74}. Examples from human pathogens are the export of a coat protein from EAEC contributing to bacterial dispersion, the polysaccharide-dependent adhesion of *Kingella kingae* to human ECs, and the fimbriae-mediated adhesion of *Streptococcus parasanguis*^{75–77}. Another example is protein F as part of an ABC transporter from *Haemophilus influenzae* whose N-terminus promotes binding to ECs⁷⁸.

To conclude, non-pathogenic *Listeria* species have been investigated here for the first time in a mouse model for oral infection, and the results suggest differences in the colonization ability of *Listeria sensu stricto* and *Listeria sensu lato* members. Novel *Listeria sensu stricto*-specific factors involved in the colonization of the gastrointestinal tract were identified, whereas as the *Listeria sensu lato* species seem to be less adapted to the conditions of the gastrointestinal tract. Because the non-pathogenic *Listeria* species of the *sensu stricto* group including *L. welshimeri* are equipped with these determinants, their potential to occupy niches of the pathogenic species has been underestimated.

Methods

Bacterial strains, plasmids, cell lines and growth conditions. The bacterial strains, cell lines, and plasmids used in this study are listed in Supplementary Table S2. *E. coli* was grown in Luria-Bertani broth, while *L. monocytogenes* EGDe was cultivated in BHI or MM⁵¹ at 37 °C or 24 °C. If appropriate, the media were supplemented with the following antibiotics: erythromycin (300 µg/ml for *E. coli* or 10 µg/ml for *L. monocytogenes*), kanamycin (50 µg/ml), and chloramphenicol (10 µg/ml). For solid media, 1.5% agar (w/v) was added. Human colon ECs (Caco-2 cells, ATCC HTB-37) and human larynx squamous cell carcinoma cells (HEp-2 cells, ATCC CCL-23) were received from the American Type Culture Collection and were cultured at 37 °C and 5% CO₂ in Dulbecco's Modified Eagle Medium (Biochrom KG, Berlin, Germany) supplemented with 10% fetal calf serum (Pan Biotech, Aidenbach, Germany). For RNA isolation, 50.5 ml of BHI was inoculated with 0.5 ml of a *L. monocytogenes* overnight culture and incubated at 37 °C or 24 °C with shaking (150 rpm). Aerobic growth in broth was conducted in Erlenmeyer flasks with constant shaking; anaerobic growth was performed in sealed Falcon tubes. Growth was monitored by measuring OD₆₀₀ with a Lambda Bio + spectrophotometer (Perkin Elmer, Waltham, MA, USA). If appropriate, 3.5 ml of BHI supplemented with 10 mM 1,2-PD (Sigma-Aldrich, Taufkirchen, Germany) and/or 25 nm cobalamin (Applichem, Darmstadt, Germany) in a 15-ml glass tube was inoculated with 0.25 ml of an *L. monocytogenes* overnight culture and incubated at 37 °C with shaking.

Standard procedures. DNA manipulations and isolation of chromosomal DNA were performed in accordance with standard protocols⁷⁹ and following the manufacturer's instructions. GeneRuler™ 1 kb DNA Ladder from Thermo Scientific (Waltham, MA, USA) was used as a marker for DNA analysis. A Bio-Rad Gene pulser II was used for electroporation. PCR was carried out with Taq polymerase and with 100–400 ng of chromosomal DNA or an aliquot of a single colony resuspended in 50 µl of H₂O as template. Quantitative real-time (qRT)-PCR and whole bacterial RNA isolation were performed as described recently⁸⁰. Transcription of the housekeeping gene 16S rRNA and *lmo1759* (*pcrA*) was used for normalization. The oligonucleotides used in this study are listed in

Supplementary Table S3. For listerial gene annotation, the *Listeria* homepage of the Institut Pasteur (<http://genolist.pasteur.fr/ListiList/>) was used.

For genome comparison, type strain genomic sequences of the 16 *Listeria* species were downloaded from NCBI GenBank. Sequences were uploaded to the RAST server⁸¹ and functionally annotated. *L. grayi* was excluded from this comparison since it is most closely related to *Listeria sensu stricto*, although it belongs to the *Listeria sensu lato* group.

In-frame gene deletions were performed as described recently⁶². Briefly, two flanking fragments of ~1000 bp were amplified from chromosomal DNA derived from the strain EGDe using the oligonucleotides indicated in Supplementary Table S3 and ligated *via* the introduced *Bgl*II sites. Following nested PCR and using the ligation mixture as a template, the resulting fragment was cloned into pLSV101 *via* *Sal*I and *Xma*I. Following transformation of the resulting plasmids, erythromycin-resistant EGDe harboring the chromosomally integrated plasmid were selected upon incubation at 42 °C. Cointegrates were resolved, erythromycin-sensitive clones were screened by PCR, and the deletion sites were sequenced to identify the respective mutant strains.

Transcriptome analysis. Whole-transcriptome RNA library preparation was performed as described recently⁸². Briefly, RNA was extracted, ribosomal RNAs were depleted, and RNA was fragmented *via* sonication. After dephosphorylation and rephosphorylation, TruSeq Small RNA Sample Kit (Illumina, Munich, Germany) was used, and the resulting cDNAs were size-selected. Libraries were then diluted and sequenced on a MiSeq sequencer (Illumina, Munich, Germany) using a MiSeq Reagent Kit v2 (50 cycles), resulting in 50 bp single-end reads. Illumina FASTQ files were mapped to the reference genome of *L. monocytogenes* EGDe (GenBank: NC_003210) using Bowtie for Illumina implemented in Galaxy^{83,84}. SAM files were converted to BAM files and indexed. Artemis^{85,86} was used to visualize and calculate the number of reads mapping on each gene. Gene counts of each library were normalized to the smallest library in the comparison and RPKM (reads per kilobase per million mapped reads) values were calculated. Fold changes between the different conditions were calculated and visualized using a three-color scheme.

EC adhesion and invasion assays. A total of 2.5×10^5 Caco-2 or HEp-2 cells per well were seeded in a 24-well culture plate and cultivated for 48 h until infection. Cells were washed twice with PBS/Mg²⁺Ca²⁺ and covered for 35 min (adhesion assay) or 1 h (invasion assay) with 500 µl of DMEM containing approximately 2.5×10^6 bacteria (multiplicity of infection, MOI, =10) from a glycerol stock washed with PBS. For glycerol stocks, strains were grown in 20 ml of BHI medium to mid-log phase (OD₆₀₀ ~0.85–0.95) and supplemented with glycerol (15% final concentration). Aliquots of 1 ml were frozen at –80 °C. Prior to infection, samples were thawed, and the number of viable bacteria was determined as cfu per ml.

The average MOI was calculated immediately after infection and ranged from 8 to 11. For assessment of adhesion, the Caco-2 or HEp-2 cells were washed thrice with PBS/Mg²⁺Ca²⁺ after a 35-min incubation period. Cell layers were lysed in 1 ml of cold Triton X-100 (0.1%) and vortexed for 1 min to disrupt the cells. For invasion assays, Caco-2 or HEp-2 cells were washed twice with PBS/Mg²⁺Ca²⁺ after 1 h of incubation. Extracellular bacteria were removed by adding 0.5 ml of DMEM containing 100 µg/ml gentamycin for 1 h, and the medium was then replaced by DMEM with 10 µg/ml gentamycin. At appropriate time points of incubation in the presence of 10 µg/ml gentamycin, the infected eukaryotic cells were washed again with PBS/Mg²⁺Ca²⁺ and then lysed in 1 ml of cold Triton X-100 (0.1%) and vortexed. Adhesion and invasion characteristics as well as intracellular replication behavior of the mutants and the wild type were quantified by plating dilutions of the lysed cells on BHI agar plates that had been incubated at 37 °C for one day. In all experiments, intact eukaryotic cell monolayers were observed prior to cell lysis.

In vitro growth analyses. For growth analysis of *L. monocytogenes* EGDe and EGDe $\Delta pduD$, we used the Bioscreen C Automated Microbiology Growth Curve Analysis System (Oy Growth Curves Ab Ltd., Helsinki, Finland), allowing automated OD measurement in a microvolume of 200 µl. Overnight cultures of *L. monocytogenes* grown in BHI at 37 °C were washed with PBS and then diluted in PBS to obtain an OD₆₀₀ of 1. This cell suspension was further diluted 1:20 in MM⁵¹ containing 0.5% (w/v) yeast extract (Oxoid, Wesel Germany). MM was supplemented with 0 or 50 mM glucose (Fluka, Neu-Ulm, Germany). Cultures were incubated at 37 °C with continuous medium shaking (shaking steps: 60), and were overlaid with 200 µl of paraffin oil (Roth, Karlsruhe, Germany) to establish anaerobic conditions. The OD₆₀₀ was automatically measured every 30 min over a period of 10 h.

Mouse infections. Four-week-old female BALBc/By/J mice from The Jackson Laboratory (Bar Harbor, ME, USA) or BALB/cAnNCrI mice from Charles River Laboratories (Sulzfeld, Germany) were purchased and used for experiments at the age of 6–8 weeks. Mice were maintained in a specific-pathogen-free facility with a 14-h light and 10-h dark cycle. Mice were infected using a model for foodborne infection as described previously⁴⁶. Mice were placed in a cage with raised wire flooring to prevent coprophagy and denied food for 18–22 h before the infection. Aliquots of frozen *L. monocytogenes* or other *Listeria* species were recovered in BHI medium for 1.5 h at 30 °C without shaking. The desired inoculum was resuspended in 2 µl of PBS mixed with 3 µl of salted butter (Kroger, Cincinnati, OH, USA or REWE, Cologne, Germany). Cell suspension was used to saturate a 2- to 3-mm piece of bread (Kroger or REWE). After the onset of the dark cycle, mice were transferred to an empty cage and fed the *Listeria*-contaminated pieces of bread with sterile forceps. Afterwards, the mice were returned to their raised wire flooring cages and mouse chow was replenished. Sample collection and handling was performed as described recently⁴⁶. We confirm that all methods were carried out in accordance with relevant guidelines and regulations, and that all experimental protocols were approved by the Regierung von Oberbayern, München, Germany.

Statistics. Statistical analyses for all experiments were performed using the Student's *t*-Test with Welch's correction in Prism6 (GraphPad, La Jolla, CA, USA). *P* values less than 0.05 were considered significant and are indicated as follows: *(*P* < 0.05); **(*P* < 0.01); ***(*P* < 0.001); NS (not significant, *P* ≥ 0.05).

References

- Farber, J. M. & Peterkin, P. I. *Listeria monocytogenes*, a food-borne pathogen. *Microbiol Rev* **55**, 476–511 (1991).
- Collins, M. D. *et al.* Phylogenetic analysis of the genus *Listeria* based on reverse transcriptase sequencing of 16S rRNA. *Int J Syst Bacteriol* **41**, 240–246 (1991).
- Sallen, B., Rajoharison, A., Desvarenne, S., Quinn, F. & Mabilat, C. Comparative analysis of 16S and 23S rRNA sequences of *Listeria* species. *Int J Syst Bacteriol* **46**, 669–674 (1996).
- Freitag, N. E., Port, G. C. & Miner, M. D. *Listeria monocytogenes* - from saprophyte to intracellular pathogen. *Nat Rev Microbiol* **7**, 623–628 (2009).
- Thevenot, D., Dernburg, A. & Vernozy-Rozand, C. An updated review of *Listeria monocytogenes* in the pork meat industry and its products. *J Appl Microbiol* **101**, 7–17 (2006).
- Gandhi, M. & Chikindas, M. L. *Listeria*: A foodborne pathogen that knows how to survive. *Int J Food Microbiol* **113**, 1–15 (2007).
- Carpentier, B. & Cerf, O. Review—Persistence of *Listeria monocytogenes* in food industry equipment and premises. *Int J Food Microbiol* **145**, 1–8 (2011).
- Cossart, P. & Toledo-Arana, A. *Listeria monocytogenes*, a unique model in infection biology: an overview. *Microbes Infect* **10**, 1041–1050 (2008).
- Swaminathan, B. & Gerner-Smidt, P. The epidemiology of human listeriosis. *Microbes Infect* **9**, 1236–1243 (2007).
- Chaturongakul, S., Raengpradub, S., Wiedmann, M. & Boor, K. J. Modulation of stress and virulence in *Listeria monocytogenes*. *Trends Microbiol* **16**, 388–396 (2008).
- Gray, M. J., Freitag, N. E. & Boor, K. J. How the bacterial pathogen *Listeria monocytogenes* mediates the switch from environmental Dr. Jekyll to pathogenic Mr. Hyde. *Infect Immun* **74**, 2505–2512 (2006).
- Sue, D., Fink, D., Wiedmann, M. & Boor, K. J. sigmaB-dependent gene induction and expression in *Listeria monocytogenes* during osmotic and acid stress conditions simulating the intestinal environment. *Microbiology* **150**, 3843–3855 (2004).
- Kazmierczak, M. J., Mithoe, S. C., Boor, K. J. & Wiedmann, M. *Listeria monocytogenes* sigma B regulates stress response and virulence functions. *J Bacteriol* **185**, 5722–5734 (2003).
- Neuhaus, K., Satorhelyi, P., Schauer, K., Scherer, S. & Fuchs, T. M. Acid shock of *Listeria monocytogenes* at low environmental temperatures induces prfA, epithelial cell invasion, and lethality towards *Caenorhabditis elegans*. *BMC Genomics* **14**, 285 (2013).
- Scotti, M., Monzo, H. J., Lacharme-Lora, L., Lewis, D. A. & Vazquez-Boland, J. A. The PrfA virulence regulon. *Microbes Infect* **9**, 1196–1207 (2007).
- Seeliger, H. P. R., Rocourt, J., Schrettenbrunner, A., Grimont, P. A. D. & Jones, D. Notes: *Listeria ivanovii* sp. nov. *Int J Syst Evol Microbiol* **34**, 336–337 (1984).
- Cummins, J., Casey, P. G., Joyce, S. A. & Gahan, C. G. A mariner transposon-based signature-tagged mutagenesis system for the analysis of oral infection by *Listeria monocytogenes*. *PLoS One* **8**, e75437 (2013).
- Guillet, C. *et al.* Human listeriosis caused by *Listeria ivanovii*. *Emerg Infect Dis* **16**, 136–138 (2010).
- Alexander, A. V., Walker, R. L., Johnson, B. J., Charlton, B. R. & Woods, L. W. Bovine abortions attributable to *Listeria ivanovii*: four cases (1988–1990). *J Am Vet Med Assoc* **200**, 711–714 (1992).
- Chand, P. & Sadana, J. R. Outbreak of *Listeria ivanovii* abortion in sheep in India. *Vet Rec* **145**, 83–84 (1999).
- Graves, L. M. *et al.* *Listeria marthii* sp. nov., isolated from the natural environment, Finger Lakes National Forest. *Int J Syst Evol Microbiol* **60**, 1280–1288 (2010).
- Chiara, M. *et al.* Comparative Genomics of *Listeria Sensu Lato*: Genus-Wide Differences in Evolutionary Dynamics and the Progressive Gain of Complex, Potentially Pathogenicity-Related Traits through Lateral Gene Transfer. *Genome Biol Evol* **7**, 2154–2172 (2015).
- Rocourt, J. & Seeliger, H. P. Distribution of species of the genus *Listeria*. *Zentralbl Bakteriell Mikrobiol Hyg A* **259**, 317–330 (1985).
- Nayak, D. N., Savalia, C. V., Kalyani, I. H., Kumar, R. & Kshirsagar, D. P. Isolation, identification, and characterization of *Listeria* spp. from various animal origin foods. *Vet World* **8**, 695–701 (2015).
- Dahshan, H., Merwad, A. M. & Mohamed, T. S. *Listeria* Species in Broiler Poultry Farms: Potential Public Health Hazards. *J Microbiol Biotechnol* **26**, 1551–1556 (2016).
- Huang, B. *et al.* Comparison of multiplex PCR with conventional biochemical methods for the identification of *Listeria* spp. isolates from food and clinical samples in Queensland, Australia. *J Food Prot* **70**, 1874–1880 (2007).
- Husu, J. R. Epidemiological studies on the occurrence of *Listeria monocytogenes* in the feces of dairy cattle. *Zentralbl Veterinarmed B* **37**, 276–282 (1990).
- Bertsch, D. *et al.* *Listeria fleischmannii* sp. nov., isolated from cheese. *Int J Syst Evol Microbiol* **63**, 526–532 (2013).
- Lang Halter, E., Neuhaus, K. & Scherer, S. *Listeria weihenstephanensis* sp. nov., isolated from the water plant *Lemna trisulca* taken from a freshwater pond. *Int J Syst Evol Microbiol* **63**, 641–647 (2013).
- Leclercq, A. *et al.* *Listeria rocourtiae* sp. nov. *Int J Syst Evol Microbiol* **60**, 2210–2214 (2010).
- den Bakker, H. C. *et al.* *Listeria floridensis* sp. nov., *Listeria aquatica* sp. nov., *Listeria cornellensis* sp. nov., *Listeria riparia* sp. nov. and *Listeria grandensis* sp. nov., from agricultural and natural environments. *Int J Syst Evol Microbiol* **64**, 1882–1889 (2014).
- Weller, D., Andrus, A., Wiedmann, M. & den Bakker, H. C. *Listeria booriae* sp. nov. and *Listeria newyorkensis* sp. nov., from food processing environments in the USA. *Int J Syst Evol Microbiol* **65**, 286–292 (2015).
- Hof, H. & Hefner, P. Pathogenicity of *Listeria monocytogenes* in comparison to other *Listeria* species. *Infection* **16**(Suppl 2), S141–144 (1988).
- Rost, B. Twilight zone of protein sequence alignments. *Protein Eng* **12**, 85–94 (1999).
- Orsi, R. H. & Wiedmann, M. Characteristics and distribution of *Listeria* spp., including *Listeria* species newly described since 2009. *Appl Microbiol Biotechnol* **100**, 5273–5287 (2016).
- Bigot, A. *et al.* Role of FliF and FliH of *Listeria monocytogenes* in flagellar assembly and pathogenicity. *Infect Immun* **73**, 5530–5539 (2005).
- Gründling, A., Burrack, L. S., Bouwer, H. G. & Higgins, D. E. *Listeria monocytogenes* regulates flagellar motility gene expression through MogR, a transcriptional repressor required for virulence. *Proc Natl Acad Sci USA* **101**, 12318–12323 (2004).
- Dons, L. *et al.* Role of flagellin and the two-component CheA/CheY system of *Listeria monocytogenes* in host cell invasion and virulence. *Infect Immun* **72**, 3237–3244 (2004).
- Bergmann, S., Rohde, M., Schughart, K. & Lengeling, A. The bioluminescent *Listeria monocytogenes* strain Xen32 is defective in flagella expression and highly attenuated in orally infected BALB/c mice. *Gut Pathog* **5**, 19 (2013).
- O'Neil, H. S. & Marquis, H. *Listeria monocytogenes* flagella are used for motility, not as adhesins, to increase host cell invasion. *Infect Immun* **74**, 6675–6681 (2006).
- Knudsen, G. M., Olsen, J. E. & Dons, L. Characterization of DegU, a response regulator in *Listeria monocytogenes*, involved in regulation of motility and contributes to virulence. *FEMS Microbiol Lett* **240**, 171–179 (2004).

42. Borezee, E., Pellegrini, E., Beretti, J. L. & Berche, P. SvpA, a novel surface virulence-associated protein required for intracellular survival of *Listeria monocytogenes*. *Microbiology* **147**, 2913–2923 (2001).
43. Newton, S. M. *et al.* The *svpA-srtB* locus of *Listeria monocytogenes*: fur-mediated iron regulation and effect on virulence. *Mol Microbiol* **55**, 927–940 (2005).
44. Schauer, K. *et al.* Deciphering the intracellular metabolism of *Listeria monocytogenes* by mutant screening and modelling. *BMC Genomics* **11**, 573 (2010).
45. Chen, L. H. *et al.* Cyclic di-GMP-dependent signaling pathways in the pathogenic Firmicute *Listeria monocytogenes*. *PLoS Pathog* **10**, e1004301 (2014).
46. Bou Ghanem, E. N., Myers-Morales, T. & D’Orazio, S. E. A mouse model of foodborne *Listeria monocytogenes* infection. *Curr Protoc Microbiol* **31**, 9B 3 1–9B 3 16 (2013).
47. Becattini, S. *et al.* Commensal microbes provide first line defense against *Listeria monocytogenes* infection. *J Exp Med* **214**, 1973–1989 (2017).
48. Winter, S. E. *et al.* Gut inflammation provides a respiratory electron acceptor for *Salmonella*. *Nature* **467**, 426–429 (2010).
49. Srikumar, S. & Fuchs, T. M. Ethanolamine utilization contributes to proliferation of *Salmonella enterica* serovar Typhimurium in food and in nematodes. *Appl Environ Microbiol* **77**, 281–290 (2011).
50. Faber, F. *et al.* Respiration of Microbiota-Derived 1,2-propanediol Drives *Salmonella* Expansion during Colitis. *PLoS Pathog* **13**, e1006129 (2017).
51. Premaratne, R. J., Lin, W. J. & Johnson, E. A. Development of an improved chemically defined minimal medium for *Listeria monocytogenes*. *Appl Environ Microbiol* **57**, 3046–3048 (1991).
52. Roth, J. R., Lawrence, J. G. & Bobik, T. A. Cobalamin (coenzyme B12): synthesis and biological significance. *Annu Rev Microbiol* **50**, 137–181 (1996).
53. Schmid, M. W. *et al.* Evolutionary history of the genus *Listeria* and its virulence genes. *Syst Appl Microbiol* **28**, 1–18 (2005).
54. Buchrieser, C. Biodiversity of the species *Listeria monocytogenes* and the genus *Listeria*. *Microbes Infect* **9**, 1147–1155 (2007).
55. Wang, Y. *et al.* Isolation and characterization of *Listeria* species from rodents in natural environments in China. *Emerg Microbes Infect* **6**, e44 (2017).
56. Jones, G. S. *et al.* Intracellular *Listeria monocytogenes* comprises a minimal but vital fraction of the intestinal burden following foodborne infection. *Infect Immun* **83**, 3146–3156 (2015).
57. Gaillard, J. L., Berche, P., Frehel, C., Gouin, E. & Cossart, P. Entry of *L. monocytogenes* into cells is mediated by internalin, a repeat protein reminiscent of surface antigens from Gram-positive cocci. *Cell* **65**, 1127–1141 (1991).
58. Lecuit, M. *et al.* A single amino acid in E-cadherin responsible for host specificity towards the human pathogen *Listeria monocytogenes*. *EMBO J* **18**, 3956–3963 (1999).
59. Quereda, J. J., Meza-Torres, J., Cossart, P. & Pizarro-Cerda, J. Listeriolysin S: A bacteriocin from epidemic *Listeria monocytogenes* strains that targets the gut microbiota. *Gut Microbes* 1–8 (2017).
60. Fuchs, T. M., Eisenreich, W., Kern, T. & Dandekar, T. Towards a systemic understanding of *Listeria monocytogenes* metabolism during infection. *Front Microbiol* **3**, 137–143 (2012).
61. Chico-Calero, I. *et al.* Hpt, a bacterial homolog of the microsomal glucose- 6-phosphate translocase, mediates rapid intracellular proliferation in *Listeria*. *Proc Natl Acad Sci USA* **99**, 431–436 (2002).
62. Joseph, B. *et al.* Identification of *Listeria monocytogenes* genes contributing to intracellular replication by expression profiling and mutant screening. *J Bacteriol* **188**, 556–568 (2006).
63. Grubmüller, S., Schauer, K., Goebel, W., Fuchs, T. M. & Eisenreich, W. Analysis of carbon substrates used by *Listeria monocytogenes* during growth in J774A.1 macrophages suggests a bipartite intracellular metabolism. *Front Cell Infect Microbiol* **4**, 1–14 (2014).
64. Schauer, K., Stolz, J., Scherer, S. & Fuchs, T. M. Both thiamine uptake and biosynthesis of thiamine precursors are required for intracellular replication of *Listeria monocytogenes*. *J Bacteriol* **191**, 2218–2227 (2009).
65. Kutzner, E., Kern, T., Felsl, A., Eisenreich, W. & Fuchs, T. M. Isotopologue profiling of the listerial N-metabolism. *Mol Microbiol* **100**, 315–327 (2016).
66. Conner, C. P., Heithoff, D. M., Julio, S. M., Sinsheimer, R. L. & Mahan, M. J. Differential patterns of acquired virulence genes distinguish *Salmonella* strains. *Proc Natl Acad Sci USA* **95**, 4641–4645 (1998).
67. Klumpp, J. & Fuchs, T. M. Identification of novel genes in genomic islands that contribute to *Salmonella typhimurium* replication in macrophages. *Microbiology* **153**, 1207–1220 (2007).
68. Xue, J., Murrieta, C. M., Rule, D. C. & Miller, K. W. Exogenous or L-rhamnose-derived 1,2-propanediol is metabolized via a pduD-dependent pathway in *Listeria innocua*. *Appl Environ Microbiol* **74**, 7073–7079 (2008).
69. Toledo-Arana, A. *et al.* The *Listeria* transcriptional landscape from saprophytism to virulence. *Nature* **459**, 950–956 (2009).
70. Staib, L. & Fuchs, T. M. From food to cell: nutrient exploitation strategies of enteropathogens. *Microbiology* **160**, 1020–1039 (2014).
71. Gill, S. R. *et al.* Metagenomic analysis of the human distal gut microbiome. *Science* **312**, 1355–1359 (2006).
72. Wilkens, S. Structure and mechanism of ABC transporters. *PI000Prime Rep* **7**, 14 (2015).
73. Ito, Y., Kanamaru, K., Taniguchi, N., Miyamoto, S. & Tokuda, H. A novel ligand bound ABC transporter, LolCDE, provides insights into the molecular mechanisms underlying membrane detachment of bacterial lipoproteins. *Mol Microbiol* **62**, 1064–1075 (2006).
74. Fisher, M. L., Allen, R., Luo, Y. & Curtiss, R. 3rd Export of extracellular polysaccharides modulates adherence of the *Cyanobacterium synechocystis*. *PLoS One* **8**, e74514 (2013).
75. Nishi, J. *et al.* The export of coat protein from enteroaggregative *Escherichia coli* by a specific ATP-binding cassette transporter system. *J Biol Chem* **278**, 45680–45689 (2003).
76. Porsch, E. A., Kehl-Fie, T. E. & St Geme, J. W. 3rd. Modulation of *Kingella kingae* adherence to human epithelial cells by type IV Pili, capsule, and a novel trimeric autotransporter. *MBio* **3** (2012).
77. Fenno, J. C., Shaikh, A., Spatafora, G. & Fives-Taylor, P. The *fimA* locus of *Streptococcus parasanguis* encodes an ATP-binding membrane transport system. *Mol Microbiol* **15**, 849–863 (1995).
78. Jalalvand, F. *et al.* *Haemophilus influenzae* protein F mediates binding to laminin and human pulmonary epithelial cells. *J Infect Dis* **207**, 803–813 (2013).
79. Sambrook, J. & Russell, D. W. Molecular cloning: a laboratory manual, 3rd ed. Cold Spring Harbor Laboratory, Cold Spring Harbor, N. Y. (2001).
80. Muller-Herbst, S. *et al.* Identification of genes essential for anaerobic growth of *Listeria monocytogenes*. *Microbiology* **160**, 752–765 (2014).
81. Overbeek, R. *et al.* The SEED and the Rapid Annotation of microbial genomes using Subsystems Technology (RAST). *Nucleic Acid Res* **42**(Database issue), D206–14 (2014).
82. Landstorfer, R. *et al.* Comparison of strand-specific transcriptomes of enterohemorrhagic *Escherichia coli* O157:H7 EDL933 (EHEC) under eleven different environmental conditions including radish sprouts and cattle feces. *BMC Genomics* **15**, 353 (2014).
83. Goecks, J., Nekrutenko, A., Taylor, J. & Galaxy, T. Galaxy: a comprehensive approach for supporting accessible, reproducible, and transparent computational research in the life sciences. *Genome Biol* **11**, R86 (2010).
84. Blankenberg, D. *et al.* Galaxy: a web-based genome analysis tool for experimentalists. *Curr Protoc Mol Biol* Chapter 19, Unit19 10 11–21 (2010).
85. Rutherford, K. *et al.* Artemis: sequence visualization and annotation. *Bioinformatics* **16**, 944–945 (2000).

86. Carver, T., Bohme, U., Otto, T. D., Parkhill, J. & Berriman, M. BamView: viewing mapped read alignment data in the context of the reference sequence. *Bioinformatics* **26**, 676–677 (2010).
87. Camejo, A. *et al.* *In vivo* transcriptional profiling of *Listeria monocytogenes* and mutagenesis identify new virulence factors involved in infection. *PLoS Pathog* **5**, e1000449 (2009).
88. Williams, T., Bauer, S., Beier, D. & Kuhn, M. Construction and characterization of *Listeria monocytogenes* mutants with in-frame deletions in the response regulator genes identified in the genome sequence. *Infect Immun* **73**, 3152–3159 (2005).
89. Shen, A. & Higgins, D. E. The MogR transcriptional repressor regulates nonhierarchal expression of flagellar motility genes and virulence in *Listeria monocytogenes*. *PLoS Pathog* **2**, e30 (2006).
90. Begley, M. *et al.* The interplay between classical and alternative isoprenoid biosynthesis controls gammadelta T cell bioactivity of *Listeria monocytogenes*. *FEBS Lett* **561**, 99–104 (2004).
91. Iurov, D. S. *et al.* Contribution of L,D-carboxypeptidases in virulence of facultative intracellular pathogenic bacteria *Listeria monocytogenes*. *Zh Mikrobiol Epidemiol Immunobiol*, 15–20 (2012).
92. Bennett, H. J. *et al.* Characterization of *relA* and *codY* mutants of *Listeria monocytogenes*: identification of the CodY regulon and its role in virulence. *Mol Microbiol* **63**, 1453–1467 (2007).
93. Mariscotti, J. F., Garcia-del Portillo, F. & Pucciarelli, M. G. The *Listeria monocytogenes* sortase-B recognizes varied amino acids at position 2 of the sorting motif. *J Biol Chem* **284**, 6140–6146 (2009).
94. Xiao, Q. *et al.* Sortase independent and dependent systems for acquisition of haem and haemoglobin in *Listeria monocytogenes*. *Mol Microbiol* **80**, 1581–1597 (2011).
95. Livak, K. J. & Schmittgen, T. D. Analysis of relative gene expression data using real-time quantitative PCR and the 2(−Delta Delta C(T)) Method. *Methods* **25**, 402–408 (2001).

Acknowledgements

This work was supported by a grant to JS within the Research Training Group (Graduiertenkolleg) 1482 of the Deutsche Forschungsgemeinschaft. We thank Lena Riedel, Michael Schneider, Melanie Schoof, Michelle Pitts and Travis Combs for the experimental support, and Ian Monk for kindly providing the plasmids pIMC3ery and pIMC3kan.

Author Contributions

Conceived and designed the experiments: J.S., S.M.H., S.E.F.D. and T.M.F.; performed the experiments: J.S., G.J. and K.S.; analysed the data: J.S., S.M.H., S.E.F.D. and T.M.F.; wrote the manuscript: J.S., S.E.F.D. and T.M.F.

Additional Information

Supplementary information accompanies this paper at <https://doi.org/10.1038/s41598-017-17570-0>.

Competing Interests: The authors declare that they have no competing interests.

Publisher's note: Springer Nature remains neutral with regard to jurisdictional claims in published maps and institutional affiliations.



Open Access This article is licensed under a Creative Commons Attribution 4.0 International License, which permits use, sharing, adaptation, distribution and reproduction in any medium or format, as long as you give appropriate credit to the original author(s) and the source, provide a link to the Creative Commons license, and indicate if changes were made. The images or other third party material in this article are included in the article's Creative Commons license, unless indicated otherwise in a credit line to the material. If material is not included in the article's Creative Commons license and your intended use is not permitted by statutory regulation or exceeds the permitted use, you will need to obtain permission directly from the copyright holder. To view a copy of this license, visit <http://creativecommons.org/licenses/by/4.0/>.

© The Author(s) 2017